

Supporting Information

An unprecedented (6,8)-connected self-penetrating network based on two distinct zinc clusters

Ya-Qian Lan, Xin-Long Wang, Shun-Li Li, Zhong-Min Su,* Kui-Zhan Shao
and En-Bo Wang *

Institute of Functional Material Chemistry; Key Lab of Polyoxometalate Science of Ministry of Education, Faculty of Chemistry, Northeast Normal University, Changchun, 130024, China. E-mail: zmsu@nenu.edu.cn; wangenbo@public.cc.jl.cn; Tel: +86 431 85099108

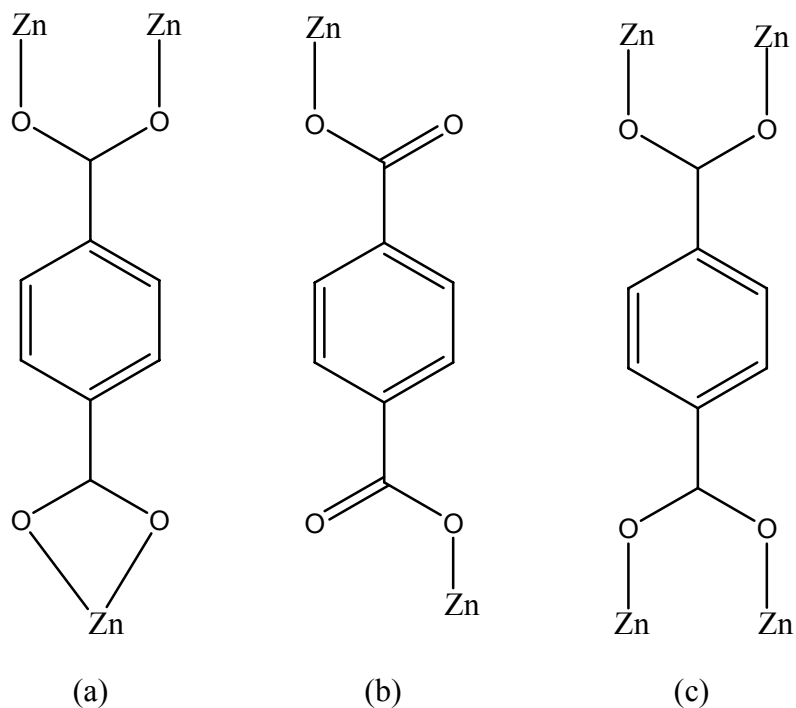
Materials. All reagents and solvents for syntheses were purchased from commercial sources and used as received.

General Characterization and Physical Measurements. The C, H, and N elemental analyses were conducted on a Perkin–Elmer 240C elemental analyzer. The FT-IR spectra was recorded from KBr pellets in the range 4000–400 cm⁻¹ on a Mattson Alpha-Centauri spectrometer. TGA was performed on a Perkin–Elmer TG-7 analyzer heated from room temperature to 800°C under nitrogen.

Synthesis of L: A mixture of 3-hydroxypyridine (4.755 g, 50 mmol) and NaOH (1.00 g, 25 mmol) in DMF (20 mL) was stirred at 60 °C for 1 h, and the 4,4'-bis(chloromethyl)biphenyl (6.28 g, 25 mmol) was added. The mixture was cooled to room temperature after stirring at 60 °C for 24 h and then poured into 200 mL of water. A yellow solid formed immediately, which was isolated by filtration after

drying in air. The crude product was further purified on a silica column using a 2:1 aether and petroleum ether mixture (v/v). Yield: 23.1%. Elemental analyses calcd for C₂₄H₂₀N₂O₂ (368.43): C, 78.24; H, 5.47; N, 7.60%. Found: C, 78.20; H, 5.49; N, 7.60 %. IR (cm⁻¹): 3377 (s), 1570 (s), 1500 (s), 1477 (m), 1270 (s), 1231 (s), 1195 (m), 1000 (m), 805 (s), 770 (m), 708 (w).

X-ray crystallographic analysis of 1: The data were collected at 298(2) K a Bruker Apex CCD diffractometer with graphite-monochromated MoK_α radiation ($\lambda = 0.71073 \text{ \AA}$). All the structures were solved by Direct Method of SHELXS-97¹ and refined by full-matrix least-squares techniques using the SHELXL-97² program within WINGX.³ Non-hydrogen atoms were refined with anisotropic temperature parameters. The hydrogen atoms of the organic ligands were refined as rigid groups. It was found that the water molecule was equally disordered over two adjacent sites. It was not possible to locate the water H atoms.



Scheme S1. Coordination modes of the bdc ligands in **1**. (a) The chelating-bidentate and bridging-bidentate coordination mode for bdc1, (b) the bis(bridging-bidentate) coordination mode for bdc2 and (c) the bis(monodentate) coordination mode for bdc3.

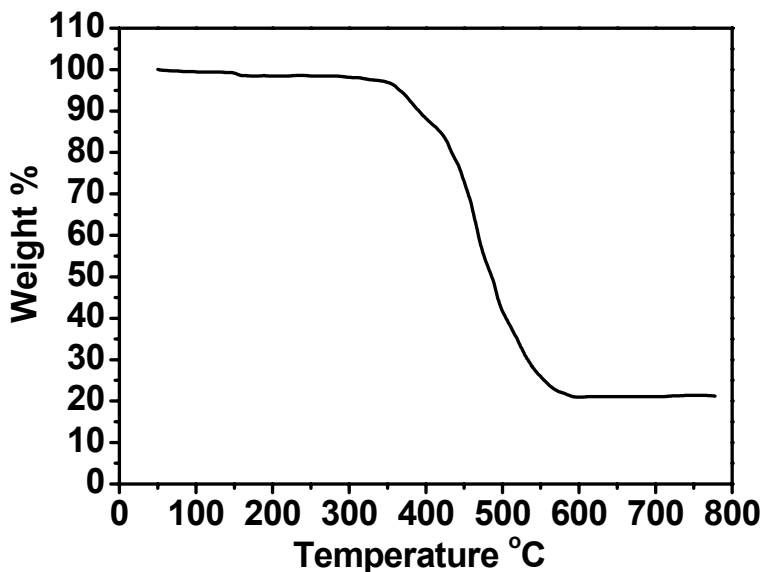


Figure S1. TGA curves of **1**.

Thermal Analysis.

In order to characterize the compound more fully in terms of thermal stability, its thermal behavior was studied by TGA. The experiment was performed on sample consisting of numerous single crystal of **1** under N₂ atmosphere with a heating rate of 10 °C/min. The weight loss corresponding to the release of one water molecule is observed from room temperature to 157 °C (obsd 1.8%, calcd 1.9%). The anhydrous [Zn_{2.5}L(bdc)_{2.5}] begins to decompose at 346 °C and ends above 596 °C. The weight loss (found: 78.9%) corresponds to the loss of water and organic components (calcd: 78.8%). The remaining weight of 21.1% corresponds to the percentage (21.2%) of Zn and O components, indicating that the final product is ZnO.

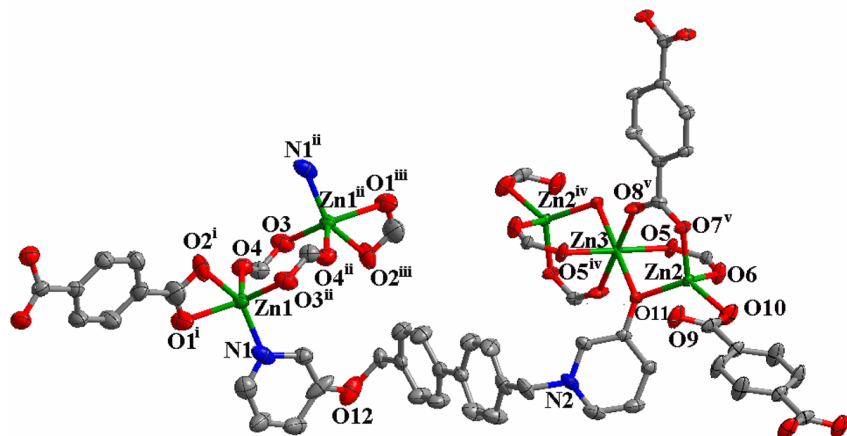


Figure S2. ORTEP view of the coordination environment Zn^{II} atoms of **1** with thermal ellipsoids at 20% probability displacement; the hydrogen atoms and water molecules are omitted for clarity. Symmetry codes: i, 1-x, y-1/2, 1/2-z; ii, 1-x, -y, 1-z; iii, 1-x, -y, 1-z; iv, -x, -y, 2-z; v, -x, y+1/2, 5/2-z.

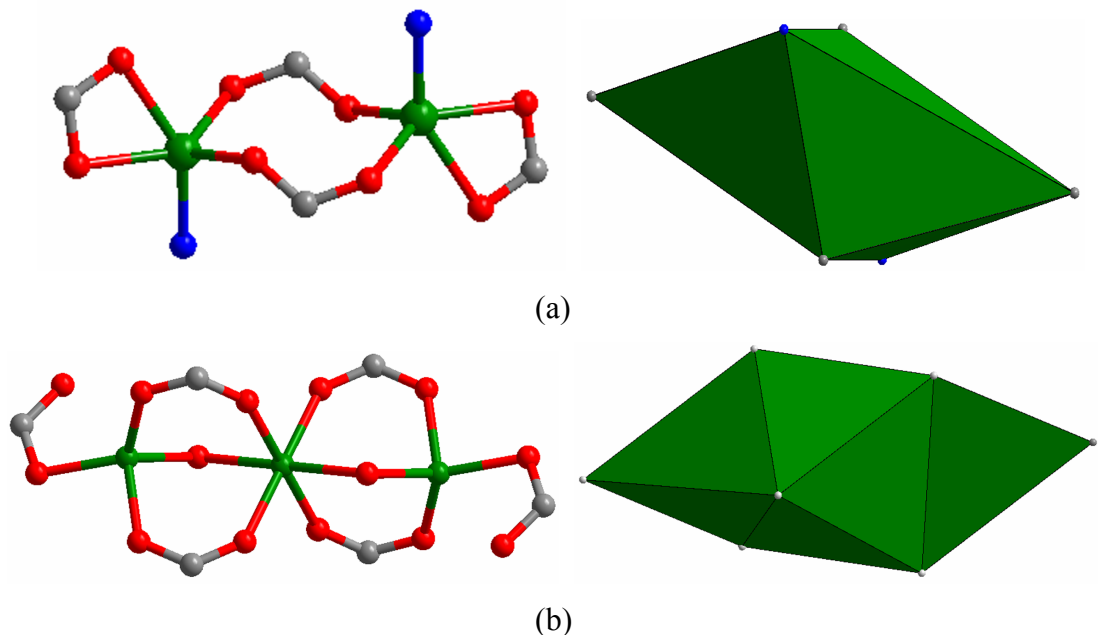


Figure S3. Ball-stick and polyhedron representations of the six-connected distorted octahedral subunit (a) and the eight-connected dodecahedral subunit (b), respectively.

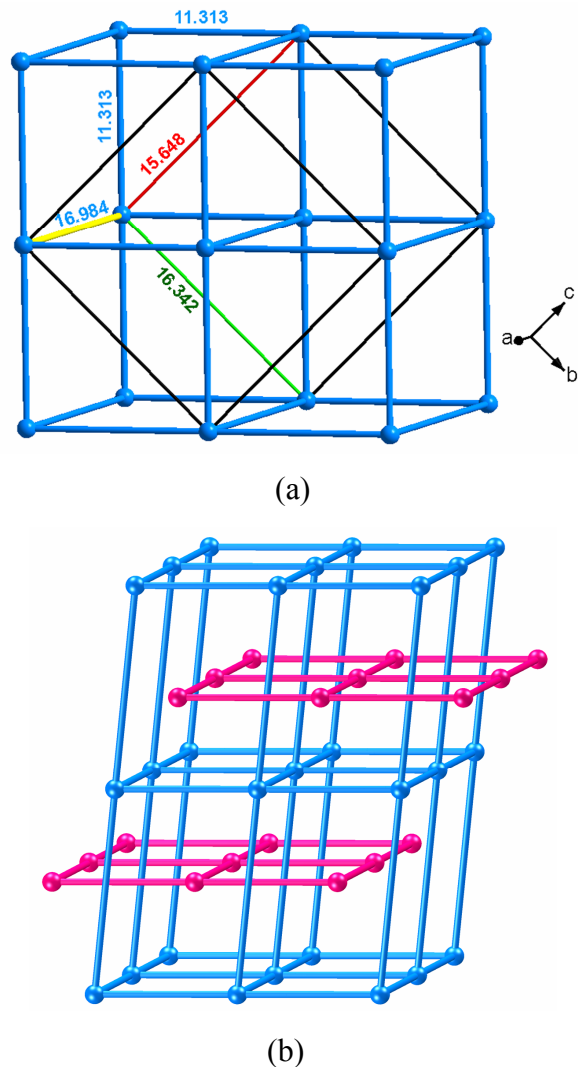


Figure S4. (a) Schematic view of the twisted α -Po topology formed by Zn2, Zn3, bdc3 and bdc3. (In the net, the crystallographically a axis and one of the edge of the α -Po net are edge-sharing, and crystallographically b and c axes are located at diagonal of the α -Po net) (b) Schematic view a 2D/3D net of the 2D layer formed by Zn1 and bdc1 penetrating the 3D twisted α -Po framework.

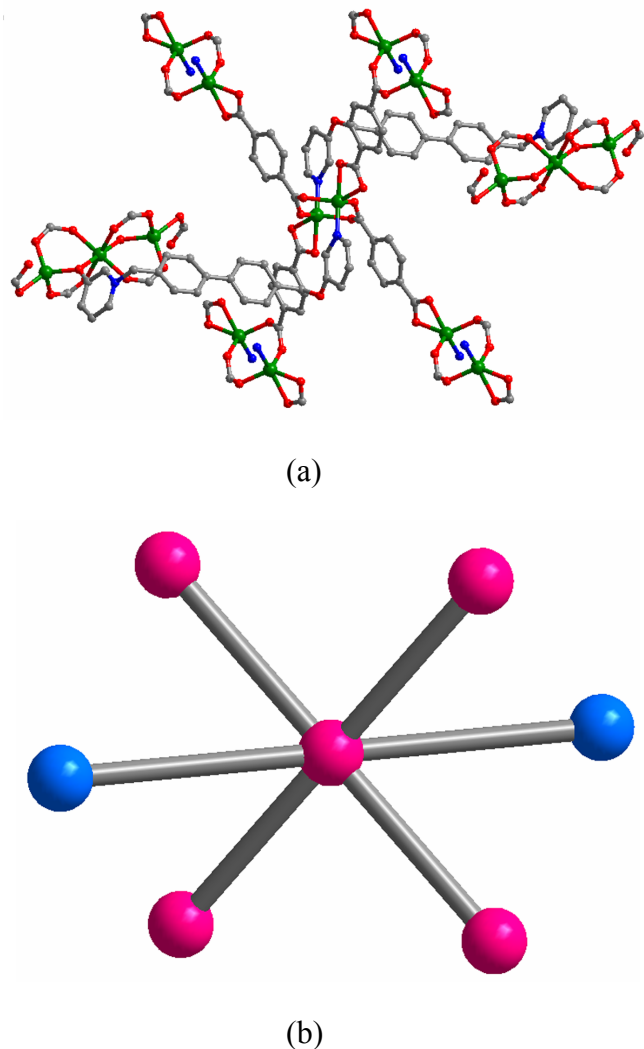


Figure S5. Ball-stick (a) and simplified (b) views of the linkages of a dinuclear zinc cluster with six adjacent clusters. (Two types of nodes are differentiated by color: blue balls refer to eight-connected nodes and pink ones refer to six-connected nodes in (b).)

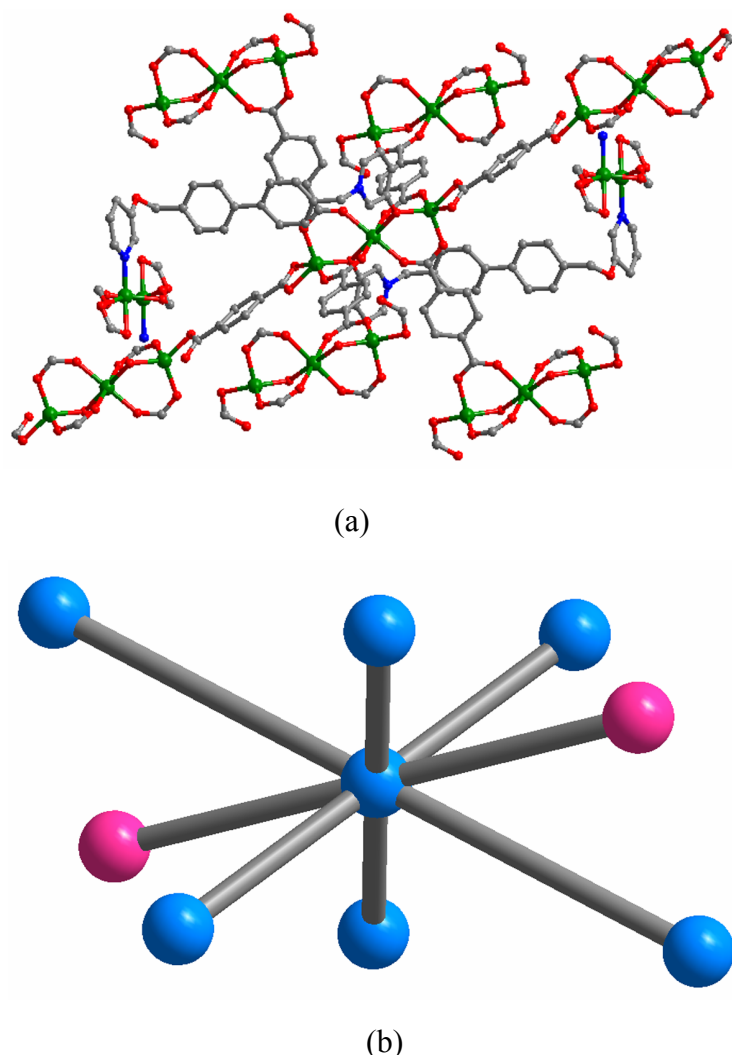


Figure S6. Ball-stick (a) and simplified (b) views of the linkages of a trinuclear zinc cluster with eight adjacent clusters. (Two types of nodes are differentiated by color: blue balls refer to eight-connected nodes and pink ones refer to six-connected nodes in (b).)

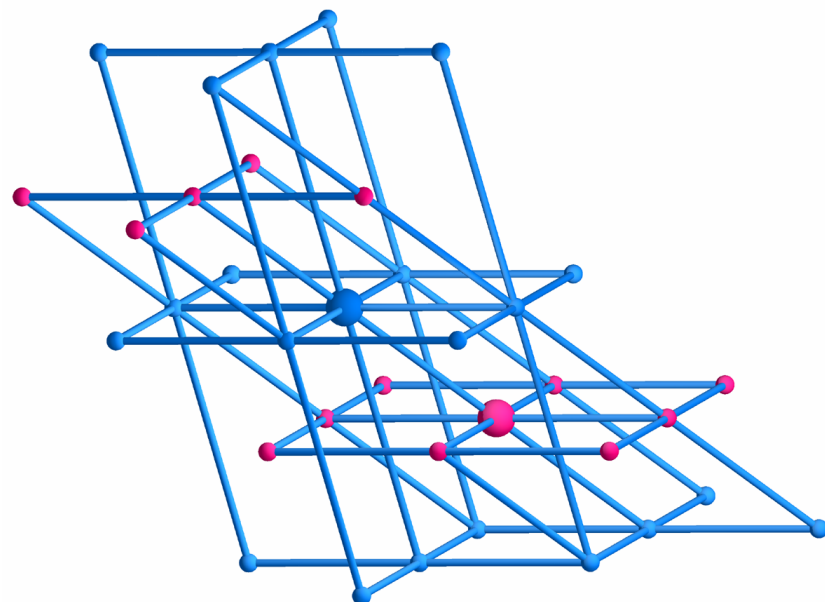


Figure S7. Schematic diagram (OLEX) showing the $(4^{12}.5.6^2)(4^{20}.5^2.6^6)$ network.
(Pink and blue balls represent six-connected nodes and eight-connected nodes,
respectively.)

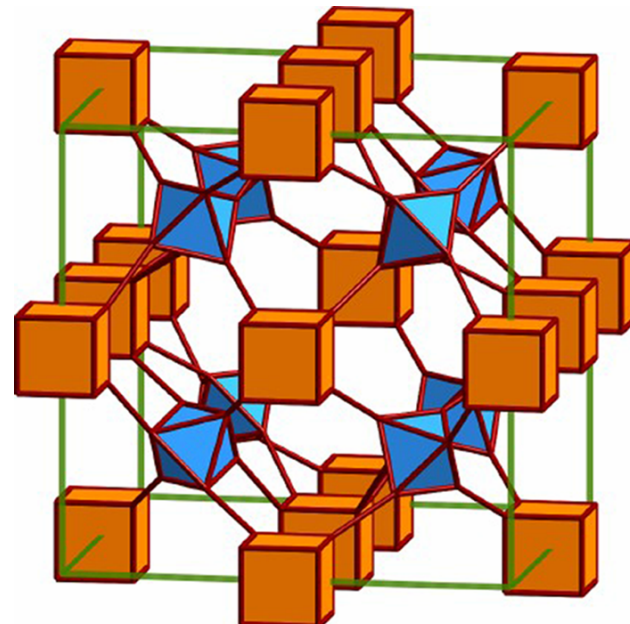


Figure S8. Polyhedron representation of the ocu topology.

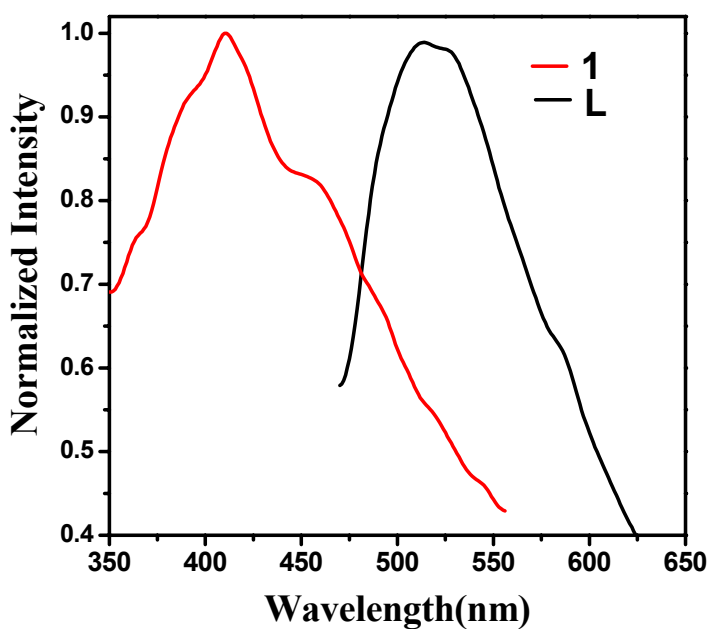


Figure S9. Emission spectra of **1** and L in the solid state at room temperature.

References

- 1 G. M. Sheldrick, *SHELXS-97, A Program for Automatic Solution of Crystal Structure*, University of Göttingen, Germany, 1997.
- 2 G. M. Sheldrick, *SHELXL-97, A Programs for Crystal Structure Refinement*, University of Göttingen, Germany, 1997.
- 3 L. J. Farrugia, *WINGX, A Windows Program for Crystal Structure Analysis*, University of Glasgow, Glasgow, UK, 1988.